Supplementary Information

Article title: Stalagmite stratigraphy constrains Late Holocene tephrochronology of southernmost Patagonia: High-resolution data for a super-humid environment

Authors: Björn Klaes[1,2*], Gerhard Wörner[3], Katrina Kremer[4], Klaus Simon[3], Denis Scholz[5], Carsten W. Mueller[6], Carmen Höschen[7], Julian Struck[8], Helge Wolfgang Arz[9], Sören Thiele-Bruhn[2], Daniel Schimpf[1], Rolf Kilian[1,10†]

[1]Geology Department, Trier University, Campus II (Geozentrum), Behringstraße 21, D-54296 Trier, Germany; [*]klaesb@uni-trier.de, d_schimpf@gmx.de
[2]Soil Science Department, Trier University, Campus II (Geozentrum), Behringstraße 21, D-54296 Trier, Germany; thiele@uni-trier.de
[3]Geochemistry Division, GZG, Georg-August-University Göttingen, Goldschmidtstraße 1, D-37077 Göttingen, Germany; gwoerne@gwdg.de, ksimon@gwdg.de
[4]Swiss Seismological Service, ETH Zürich, Sonneggstrasse 5, CH-8092 Zürich, Switzerland, katrina.kremer@sed.ethz.ch
[5]Institute for Geosciences, Johannes Gutenberg University Mainz, Johann-Joachim-Becher-Weg 21, D-55128 Mainz, Germany; scholzd@uni-mainz.de
[6]Department for Geosciences and Environmental Management, University of Copenhagen, Øster Voldgade 10, DK-1350 København K, Denmark; cm@ign.ku.dk
[7]Soil Science, Research Department Life Science Systems, TUM School of Life Sciences, Technical University of Munich, Emil-Ramann-Straße 2, D-85354 Freising-Weihenstephan, Germany; carmen.hoeschen@wzw.tum.de
[8]Department of Physical Geography, Friedrich-Schiller-University Jena, Löbdergraben 32, D-07743 Jena, Germany; julian.struck@uni-jena.de
[9]Marine Geology Section, Leibniz Institute for Baltic Sea Research Warnemünde (IOW), Seestraße 15, D-18119 Rostock, Germany; helge.arz@io-warnemuende.de
[10]University of Magallanes, Avenida Bulnes 01855, Punta Arenas, Chile

corresponding author (B. Klaes); [†] = deceased

Table S1: Results of the ^{230}Th/U-dating for stalagmite MA1 and the detritus-corrected ages according to Budsky et al.[1] used for the StalAge algorithm[2]. Standard deviations are given as 2σ-errors. Dft = distance from top. ^{230}Th/U dating points used in Schimpf et al.[3] are marked with *.

Lab. #	Dft [mm]	^{238}U [µg/g]	±	^{232}Th [ng/g]	±	(^{234}U/^{238}U)	±	^{230}Th/^{238}U)	±	(^{230}Th/^{232}Th)	±	Age uncorrected [kyrs BP]	±	Age corrected [kyrs BP]	±	Source
3654	7	1.6321	0.0016	0.7305	0.0045	0.9834	0.0015	0.001324	0.000083	9.04	0.57	0.0771	0.0090	0.064	0.011	*
3435	21	1.5446	0.0015	1.592	0.064	0.9813	0.0021	0.00590	0.00047	17.5	1.6	0.589	0.052	0.558	0.054	*
3922	39.75	1.7531	0.0029	6.767	0.052	0.9825	0.0028	0.00868	0.00025	6.87	0.21	0.899	0.028	0.783	0.062	*
3674	54.75	1.9697	0.0020	8.538	0.097	0.9806	0.0023	0.01089	0.00052	7.68	0.38	1.149	0.058	1.019	0.087	*
3849	74.9	1.7391	0.0018	4.298	0.015	0.9872	0.0020	0.01319	0.00021	16.31	0.26	1.399	0.023	1.325	0.044	*
3628	90	1.6934	0.0017	14.719	0.053	0.9819	0.0014	0.01621	0.00028	5.70	0.10	1.748	0.032	1.49	0.13	*
3923	103	2.4327	0.0024	12.957	0.049	0.9802	0.0015	0.01793	0.00021	10.29	0.13	1.946	0.024	1.786	0.082	*
3692	113.25	2.1444	0.0022	2.869	0.020	0.9845	0.0019	0.01871	0.00039	42.73	0.93	2.025	0.042	1.985	0.047	*
3653	139.5	2.9935	0.0030	2.0979	0.0084	0.9811	0.0015	0.02149	0.00021	93.70	0.99	2.349	0.024	2.328	0.026	*
3672	168.5	4.5294	0.0079	105.54	0.72	0.9834	0.0026	0.03246	0.00060	4.257	0.084	3.596	0.068	2.89	0.35	this paper
3629	180	4.3807	0.0044	39.94	0.10	0.9819	0.0014	0.02871	0.00019	9.624	0.067	3.171	0.022	2.90	0.14	*
3693	205.4	4.9157	0.0049	54.45	0.22	0.9854	0.0017	0.03145	0.00029	8.675	0.087	3.472	0.033	3.14	0.17	*
3747	214.4	4.9798	0.0050	79.77	0.40	0.9861	0.0017	0.03366	0.00037	6.421	0.077	3.723	0.042	3.24	0.24	*
3737	222.6	4.6313	0.0070	16.095	0.063	0.9865	0.0024	0.03280	0.00030	28.84	0.29	3.622	0.035	3.518	0.062	*
3924	232.3	3.4411	0.0034	19.726	0.088	0.9871	0.0020	0.03454	0.00036	18.41	0.21	3.820	0.041	3.648	0.093	*
3652	245.1	2.9520	0.0032	1.9435	0.0068	0.9983	0.0019	0.03528	0.00044	163.7	2.1	3.859	0.050	3.839	0.050	*
3436	268.5	1.7612	0.0018	42.36	0.34	1.0005	0.0017	0.04651	0.00064	5.909	0.094	5.128	0.071	4.42	0.36	this paper
4234	274	1.6195	0.0028	8.392	0.041	0.9872	0.0031	0.04308	0.00065	25.41	0.40	4.803	0.077	4.65	0.10	*

Fig. S1

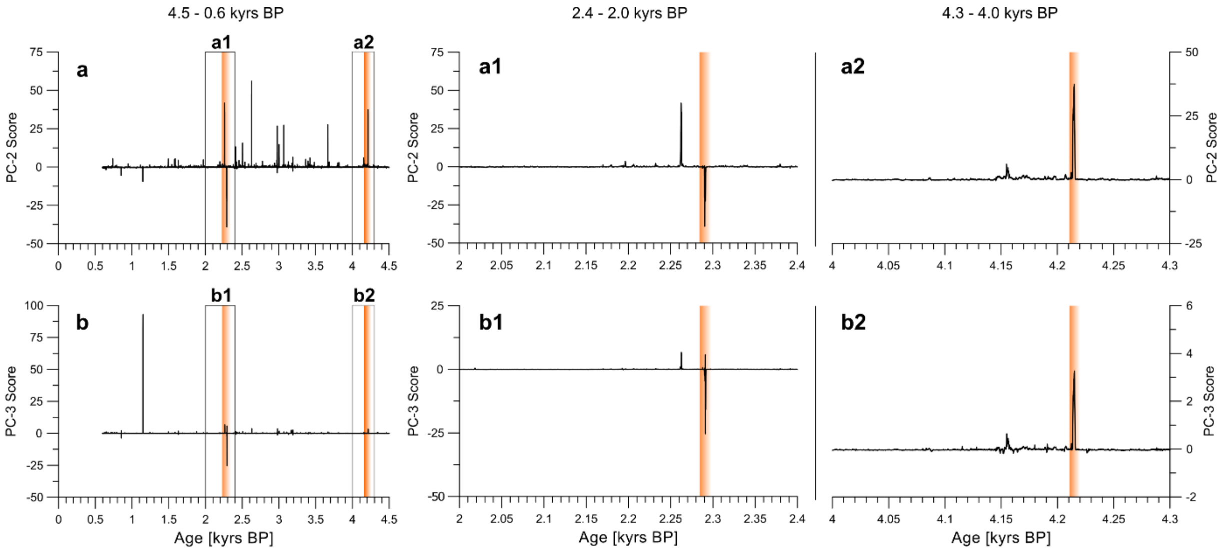

Results of the principal component analysis performed on the LA-ICP-MS data set including the six chemical elements S, P, U, Si, Sr and Zr. Panels **a** and **b** show the scores of principal components PC-2 and PC-3 for the whole time span (4.5 – 0.6 kyrs BP). Rectangles indicate the periods displayed in **a1**, **a2** and **b1**, **b2**, respectively, ranging from 4.3 – 4.0 kyrs BP and 2.4 – 2.0 kyrs BP. Orange bars mark periods at 4.216 and 2.291 kyrs BP in which PC main spikes are synchronous with trace element peaks (Figs. 3-5) and PC-1 (Fig. 6).

Table S2: **Eigenvalues and loadings of the principal component analysis.** Eigenvalues and loadings for principal components PC-1, PC-2 and PC-3 of the six variables (S, P, U, Si, Sr and Zr) are listed.

Variable	Eigenvalues	PC-1 (44.4%) Loadings	PC-2 (19.4%) Loadings	PC-3 (16.9%) Loadings
P	2.66	199.6	-12.3	-9.9
S	1.16	198.3	-12.3	-10.6
U	1.02	183.3	-12.6	11.2
Si	0.62	123.3	36.7	0.9
Sr	0.36	49.6	55.9	6.5
Zr	0.18	17.2	-5.5	92.9

47 **Fig. S2**

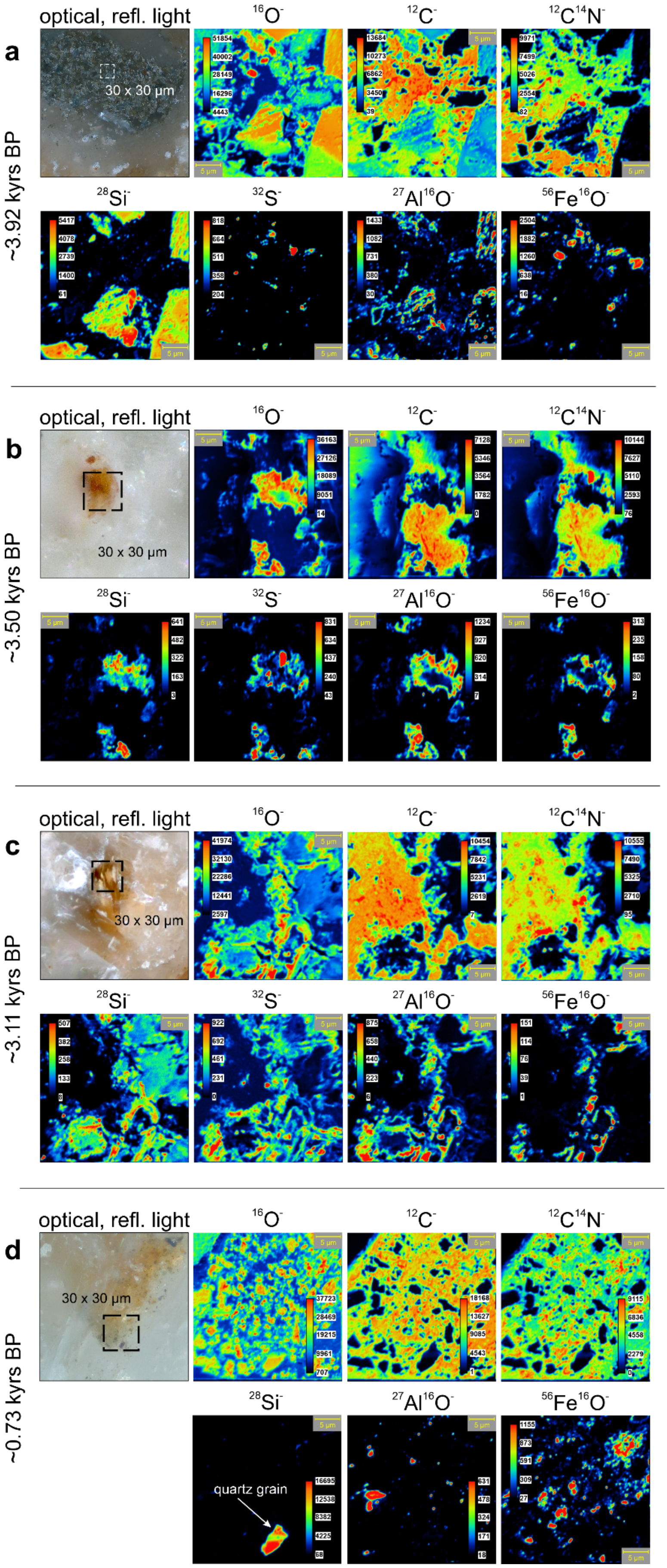
optical, refl. light
$^{16}O^-$
$^{12}C^-$
$^{12}C^{14}N^-$
a
30 x 30 µm
~3.92 kyrs BP
$^{28}Si^-$
$^{32}S^-$
$^{27}Al^{16}O^-$
$^{56}Fe^{16}O^-$
b
~3.50 kyrs BP
c
~3.11 kyrs BP
d
~0.73 kyrs BP
quartz grain

48

NanoSIMS secondary ion mappings of detritus-rich lamina at ~3.92, ~3.50, ~3.11 and ~0.73 kyrs BP. a, NanoSIMS measurements of laminae including more unweathered glass shards (~3.92 kyrs BP) in addition to Fig. 7. **b**, **c**, Residual fragments of Si-rich particles detected in laminae formed during the acidification phase after the MB_2 eruption as suggested by Kilian et al.[4]. In both cases, at ~3.50 and ~3.11 kyrs BP, secondary ion mappings of $^{28}Si^-$, $^{27}Al^{16}O^-$, $^{56}Fe^{16}O^-$ indicate that weathering residues from the catchment were incorporated together with OM ($^{12}C^-$, $^{12}C^{14}N^-$), involving strongly weathered volcanic glass. In contrast, the NanoSIMS study in **d** at ~0.73 kyrs BP depicts a lamina section containing a quartz grain. Here, $^{16}O^-$ and $^{28}Si^-$ secondary ion counts are very high whereas $^{27}Al^{16}O^-$ and $^{56}Fe^{16}O^-$ show a completely different spatial distribution compared to **a** and Fig. 7 as well as **b** and **c**.

Fig. S3

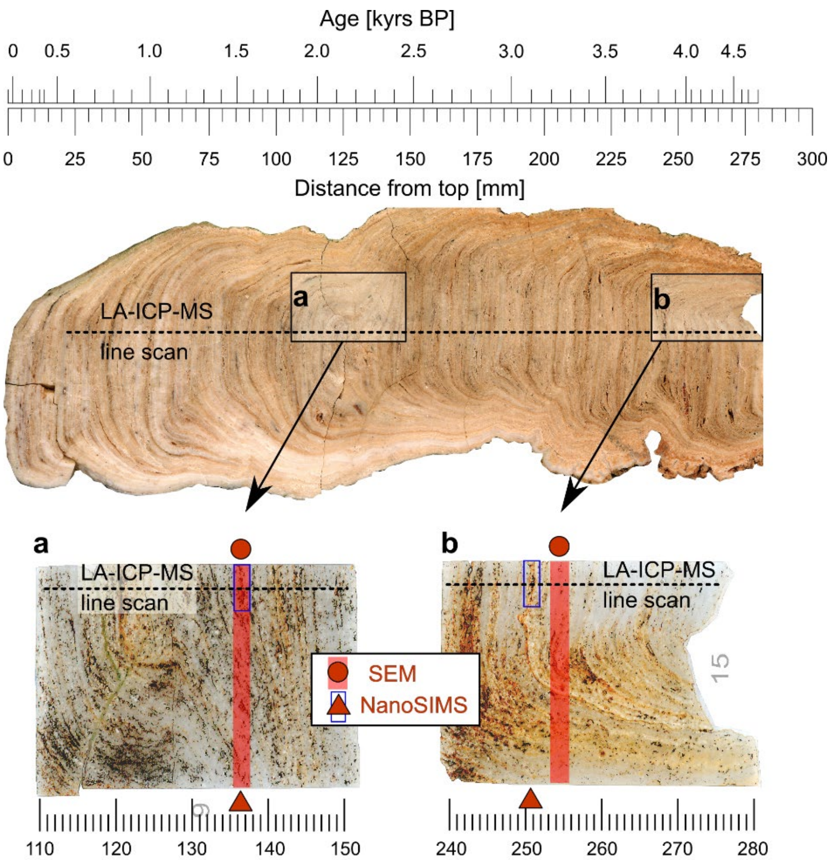

Analytical setup with exemplary thin sections. Cross-section and thin sections of the MA1 stalagmite showing the position of the LA-ICP-MS line scan measurements along the growth axis (Figs. 3-5). Two exemplary thin sections illustrate the laminae containing the signals of the Plinian Mt. Burney eruptions at 2.291 (**a**) and 4.216 (**b**) kyrs BP. Areas of interest selected for SEM and NanoSIMS investigations at 2.0 – 2.3 kyrs BP and 3.8 – 4.2 kyrs BP (Figs. 7 and S2) are also indicated.

Fig. S4

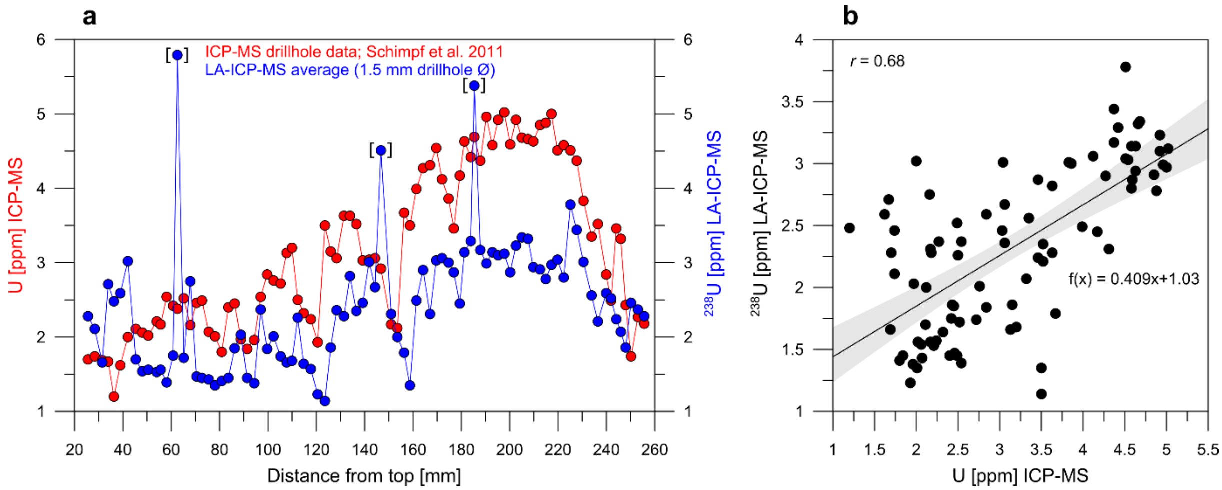

a, U concentrations deduced from ICP-MS drill core data[3] compared with average U contents determined by LA-ICP-MS (this paper) of MA1. Average U contents were calculated as an analogue to the drill core data. Here, the exact distance from top for drill core positions was considered and the used diameter of 1.5 mm[3] was applied. **b**, Relationship between ICP-MS drill core and LA-ICP-MS data with the 95% confidence interval displayed in gray. Outlier values in brackets (**a**) were excluded. Averaged LA-ICP-MS U concentrations also depict the trend of intense terrestrial leaching evoked by the long-term acidification after the MB_2 eruption[4] (240 – 160 mm distance from top).

References – Supplementary information

1. Budsky, A. et al. Speleothem record suggests enhanced summer drought in south-eastern Spain between 9.7 and 7.5 ka – a circum-Western Mediterranean anomaly? *The Holocene* **29**, 1113-1133 (2019).
2. Scholz, D. & Hoffmann, D. L. StalAge – An algorithm designed for construction of speleothem age models. *Quat. Geochron.* **6**, 369-382. (2011).
3. Schimpf, D. et al. The significance of chemical, isotopic, and detrital components in three coeval stalagmites from the superhumid southernmost Andes (53° S) as high-resolution palaeo-climate proxies. *Quat. Sci. Rev*. **30(3-4)**, 443–459 (2011).
4. Kilian, R. et al. Millennium-scale volcanic impact on a pristine and superhumid ecosystem. *Geology* **34 (8)**, 609-612 (2006).